CHAPTER 48

ESTIMATION OF INCIDENT AND REFLECTED WAVES

IN RANDOM WAVE EXPERIMENTS

by

Yoshimi Goda and Yasumasa Suzuki

Marine Hydrodynamics Division

Port and Harbour Research Institute, Ministry of Transport

Nagase, Yokosuka, Japan

ABSTRACT

A technique to resolve the incident and reflected waves from the records of composite waves is presented. It is applicable to both regular and irregular trains of waves. Two simultaneous wave records are taken at adjacent locations, and all the amplitudes of Fourier components are analyzed by the FFT technique. The amplitudes of incident and reflected wave components are estimated from the Fourier components, and the incident and reflected wave spectra are constructed by smoothing the estimated periodograms. The wave resolution is effective in the range outside the condition of the gauge spacing being even integer of half wavelength. The ratio of incident and reflected wave energies in the effective resolution range is employed in estimating the overall reflection coefficient. The incident and reflected wave heights are estimated from the composite wave heights by energy consideration.

INTRODUCTION

The importance of wave irregularity concept in coastal engineering study and application is now rightly recognized by many researchers and engineers. A rapid increase in the number of random wave generators in hydraulic laboratories in the world testifies it. With this situation, many researchers are keenly feeling the necessity of developing various experimental techniques inherent to irregular waves. Resolution of incident and reflected waves in a continuous, irregular wave system is one of the most needed techniques. If the resolution becomes feasible, then we can make tests of reflective coastal structures in continuous runs without worrying about the multi-reflection of irregular waves between a wave paddle and a reflective structure. Otherwise, we have to employ a tedious

procedure of repeating a number of short runs of different wave sequences, each of which must be stopped before the return of re-reflected waves by the wave paddle to the structure. Not only the procedure is laborious, but also the test waves are deficient in the spectral component of high frequency band due to the wave dispersion unless a special wave generation technique is employed.

The authors present a resolution technique, which involves a simultaneous recordings of wave profiles at two adjacent stations in a wave flume. The technique is similar to the one employed by Kajima [1] and by Thornton and Calhoun [2], but the use of the Fast Fourier Transform technique in yielding the Fourier components of all the frequency resolutions makes the calculation simple and versatile. For example, the technique is applicable to regular waves too, which has provided a means of calibration of resolution. The paper describes the principle of resolution technique and its accuracy with supporting data. Examples of application in the authors' experiments are also discussed.

PRINCIPLE OF RESOLUTION TECHNIQUE

Suppose we have a multi-wave-reflection system of regular waves in a wave flume. Waves generated by a wave paddle propagate forward in the flume and are reflected by a test structure. The reflected waves propagate back to the wave paddle and are re-reflected. The re-reflected waves propagate forward again and the process is repeated until the multi-reflected waves are fully attenuated. Thus the wave system can be regarded as a superposition of a number of waves propagating in the positive and negative directions of the coordinate, x (see Fig. 1). The waves propagating in each direction form a single train of progressive waves as a whole, because of the constancy of wave frequency (see Appendix). The wave train in the positive direction is called the incident waves and that in the negative direction is called the reflected waves. Let the amplitude of superposed incident waves be a_I and that of reflected waves be a_R. Then these waves are described to have the general form of

$$\left.\begin{aligned} \eta_I &= a_I \cos(kx - \sigma t + \varepsilon_I), \\ \eta_R &= a_R \cos(kx + \sigma t + \varepsilon_R), \end{aligned}\right\} \tag{1}$$

where η_I and η_R are the surface elevations of incident and reflected waves, k is the wave number of $2\pi/L$ with L being the wavelength, σ is the angular frequency of $2\pi/T$ with T being the wave period, and ε_I and ε_R are the phase angles of incident and reflected waves.
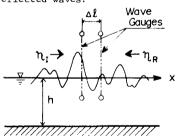

Fig. 1 Definition Sketch

Further, we suppose that the surface elevations are recorded at two adjacent stations of x_1 and $x_2 = x_1 + \Delta \ell$. The observed profiles of composite waves will be

$$
\left.
\begin{aligned}
\eta_1 &= (\eta_I + \eta_R)_{x=x_1} = A_1 \cos \sigma t + B_1 \sin \sigma t, \\
\eta_2 &= (\eta_I + \eta_R)_{x=x_2} = A_2 \cos \sigma t + B_2 \sin \sigma t,
\end{aligned}
\right\} \tag{2}
$$

where,

$$
\left.
\begin{aligned}
A_1 &= a_I \cos \phi_I + a_R \cos \phi_R, \\
B_1 &= a_I \sin \phi_I - a_R \sin \phi_R, \\
A_2 &= a_I \cos(k\Delta\ell + \phi_I) + a_R \cos(k\Delta\ell + \phi_R), \\
B_2 &= a_I \sin(k\Delta\ell + \phi_I) - a_R \sin(k\Delta\ell + \phi_R),
\end{aligned}
\right\} \tag{3}
$$

$$
\left.
\begin{aligned}
\phi_I &= kx_1 + \varepsilon_I, \\
\phi_R &= kx_1 + \varepsilon_R.
\end{aligned}
\right\} \tag{4}
$$

Equation 3 can be solved to yield the estimate of

$$
\left.
\begin{aligned}
a_I &= \frac{1}{2|\sin k\Delta\ell|} \sqrt{(A_2 - A_1 \cos k\Delta\ell - B_1 \sin k\Delta\ell)^2 + (B_2 + A_1 \sin k\Delta\ell - B_1 \cos k\Delta\ell)^2}, \\
a_R &= \frac{1}{2|\sin k\Delta\ell|} \sqrt{(A_2 - A_1 \cos k\Delta\ell + B_1 \sin k\Delta\ell)^2 + (B_2 - A_1 \sin k\Delta\ell - B_1 \cos k\Delta\ell)^2}.
\end{aligned}
\right\} \tag{5}
$$

In the calculation, the dispersion relation of the following is presumed to hold:

$$
\sigma^2 = gk \tanh kh. \tag{6}
$$

Actual wave profiles usually contain some higher harmonics. Use of the Fourier analysis enables to estimate the amplitudes of A_1, B_1, A_2, and B_2 for the fundamental frequency as well as for higher harmonics. The amplitudes of incident and reflected waves, a_I and a_R, are then estimated by Eq. 5. This is the procedure to be taken for regular wave tests.

The principle of resolution is the same for irregular waves with that for regular waves, because irregular waves can be treated as the superposition of a large number of component waves with the constant amplitudes and frequencies. The number of component waves which can be analyzed in irregular wave records is one half of the number of data sampling. By means of the Fast Fourier Transform technique, the amplitudes of A_1 to B_2 can be calculated for all the component waves and the corresponding amplitudes of a_I and a_R are estimated by Eq. 5. The spectra of incident and reflected waves can be obtained by smoothing the periodograms based on the estimates of a_I and a_R.

ESTIMATE OF INCIDENT AND REFLECTED WAVE HEIGHTS

Calibration of Resolution Technique with Regular Waves

The resolution technique was first applied to regular waves for the purpose of calibration. Trains of waves were generated in a wave flume temporarily built with a partition wall in a wave basin. At the generator side the partition wall was terminated with a gap of about 60 cm and a part of reflected waves could be dispersed into the wave basin. The wave absorber in the flume was built with crushed stone in the slope of 10 to 1. Two wave periods of 1.088 and 1.410 sec were employed. The mean wave heights were 8.98 and 9.23 cm, respectively, at the water depth of 43 cm. The spacing between two wave gauges was varied from $\Delta \ell = 10$ to 250 cm, and continuous wave records of 102.4 sec long were taken at the sampling period of $\Delta t = 1/15$ sec. The records were analyzed for the Fourier components of $f = 0$ to $f = 7.5$ Hz with the frequency resolution of $\Delta f = 0.0084$ Hz. Then, Eq. 5 was applied to estimate a_I and a_R for all the frequencies.

As expected, the resultant estimates showed clear peaks around the frequencies of $f = 0.92$ and 0.70 Hz and their harmonics. The peaks were not confined to one frequency resolution band because of wave fluctuations and signal noises; they were spread in a few neighbouring bands. Thus, the sum of the estimatated amplitudes of three to four continuous frequency bands around the peaks was employed as the representative amplitudes of incident and reflected waves. These amplitudes are plotted in Fig. 2 against the ratio of gauge spacing $\Delta \ell$ to the wavelength L. The reference amplitude, a_o, is the mean of estimated incident wave amplitudes in the range of $\Delta \ell / L < 0.4$ and $0.6 < \Delta \ell / L < 0.9$. The estimated amplitudes of a_I and a_R are seen to diverge around the relative spacing of $\Delta \ell / L = n/2$ with n = 0, 1, 2, . ., at which the devisor of Eq. 5, $\sin k \Delta \ell$, becomes null.

Figure 3 is a similar result of analysis for the case of perfect reflection with the same waves. Divergence of estimated amplitudes around $\Delta \ell / L = n/2$ is observed. The decrease of the reference amplitude a_s is considered due to the selection of test wave periods which corresponded to the antiresonance condition of the wave flume setup. (The reflective wall was located at the distance of 15 m from the wave paddle.) The divergence of estimated amplitudes is due to the amplification of noises and errors as the devisor of $\sin k \Delta \ell$ approaches 0. For the purpose of application, the zone of inaccuracy (or the effective range of resolution from the other viewpoint) needs to be specified. This will be discussed in the next section.

It is indicated in Fig. 2 that the estimates of a_I and a_R are quite stable except for the diverging zone. The estimates of a_R are several per cent of a_o, being in agreement with the characteristics of wave absorher. The estimates of a_R for the case of perfect reflection in Fig. 3 are almost equal to a_s, indicating the reflection coefficient being nearly 1.0. Additional test for a submerged, upright hreakwater with the crest submergence of 6 cm yielded the estimate of reflection coefficient of 0.44 to 0.55 (refer to Fig. 6). The conventional method of the measurement of reflection coefficient by means of nodal and antinodal wave heights yielded the reflection coefficient of 0.51 to 0.59 for this case. These estimates of a_R as a whole indicate their consistency with respect to reflecting conditions tested.
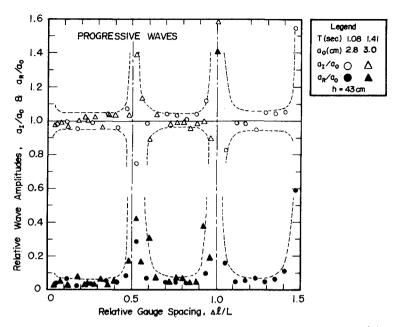
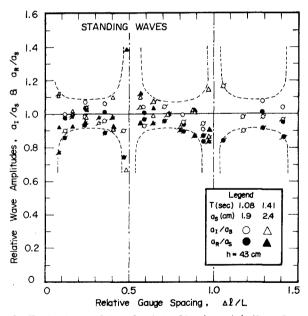Fig. 2 Variations of Resolved Amplitudes with Wave Gauge Spacing (1)

Fig. 3 Variations of Resolved Amplitudes with Wave Gauge Spacing (2)

Application for Irregular Waves

    Figure 4 is an example of spectral resolution of irregular waves.
A submerged, upright breakwater with its crest at the depth of 6 cm from
the mean water level was set at the distance of 15.0 m from the wave
paddle. The wave gauges were located at the distance of 4.80 and 5.00 m
from the breakwater face. The observed waves at the gauge locations had
the significant height of $H_{1/3}$ = 8.2 cm and period of $T_{1/3}$ = 1.44 sec.
The spectra shown in Fig. 4 are the average of three runs with the same
source spectrum but with different wave sequences. The duration of a record
was 68.3 sec and the data were sampled at the interval of 1/15 sec.
The resolved spectra of incident and reflected waves in Fig. 4 indicate
the divergence of spectral density near f = 0 and f = 1.97 Hz; the latter
frequency corresponds to the wavelength of L = 40 cm or $\Delta\ell/L$ = 0.5.
The result is a natural consequence of Figs. 2 and 3. Therefore, the resolu-
tion is effective only in some range of wave frequency. The situation is
illustrated in Fig. 5.

    There may be several methods to estimate the incident and reflected
wave heights on the basis of spectral resolution such as shown in Fig. 4.
The authors propose the following procedure. First, the effective range
of resolution is set for a given gauge spacing: in practise, the latter
is to be selected for a given wave condition. The lower and upper limits
of frequency, f_{min} and f_{max}, are better chosen by a preliminary test for
progressive waves. As a reference, the following guideline may be
consulted:

$$\left.\begin{array}{l} f_{min} : \quad \Delta\ell/L_{max} = 0.05, \\[2mm] f_{max} : \quad \Delta\ell/L_{min} = 0.45, \end{array}\right\} \tag{7}$$

where L_{max} and L_{min} are the wavelengths corresponding to f_{min} and f_{max},
respectively. Equation 7 is based on the calibration with regular waves
such as shown in Figs. 2 and 3 as well as the frequency-wise examination of
resolution results of irregular waves. There is a possibility that the
effective range may be taken slightly wider than that given by Eq. 7; e.g.,
f_{min} may be chosen so that $\Delta\ell/L_{max}$ = 0.03.

    The second step is to evaluate the energies of resolved incident and
reflected waves, E_I and E_R, contained between f_{min} and f_{max}, i.e.,

$$\left.\begin{array}{l} E_I = \displaystyle\int_{f_{min}}^{f_{max}} S_I(f)\ df, \\[4mm] E_R = \displaystyle\int_{f_{min}}^{f_{max}} S_R(f)\ df. \end{array}\right\} \tag{8}$$

The integrations are to be performed on the raw spectra of periodograms
without any smoothing to avoid the effect of divergence of resolved ampli-
tudes near $\Delta\ell/L$ = n/2.

    The third step is to estimate the overall coefficient of reflection by

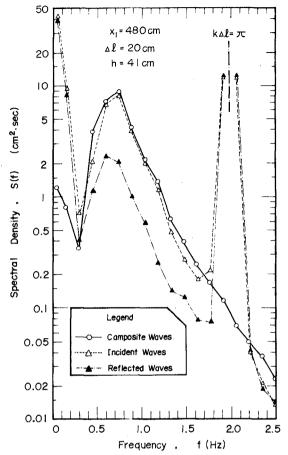$$K_R = \sqrt{E_R/E_I}. \tag{9}$$

Fig. 4   Example of Spectral Resolution for a Submerged, Upright Breakwater
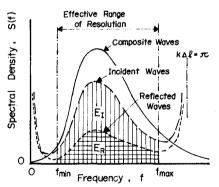

Fig. 5   Illustration of Spectral Resolution

This equation is based on the relation of irregular wave heights being proportional to the square root of wave energy. Then the incident and reflected wave heights, H_I and H_R, are calculated as

$$
\left.
\begin{aligned}
H_I &= \frac{1}{\sqrt{1 + K_R^2}}\, H_S, \\
H_R &= \frac{K_R}{\sqrt{1 + K_R^2}}\, H_S,
\end{aligned}
\right\}
\tag{10}
$$

where H_S denotes the significant or other representative wave height of composite waves observed by the two wave gauges; the mean of two gauges are employed.

Equation 10 is based on the two presumptions. The first is that the energy of composite waves appearing as the result of superposition of multiple trains of irregular waves is the sum of the energies of individual wave trains. The second is that the proportionality of representative wave heights to the square root of wave energy holds for such composite waves too, regardless of the directions of individual wave trains. The first one may be taken as an axiom for the analysis of irregular waves. The second one can be proved by a numerical simulation of irregular waves. The proof of it by the field data is almost impossible. But the applicability of the Rayleigh distribution of wave heights to ocean waves with multi-peaked spectra or the existence of the relation of $H_{1/3} \doteqdot 4.0\, \eta_{rms}$ for such waves [3,4] provides a supporting evidence for the presumption, because a multi-peaked spectrum usually indicates a coexistence of wind waves and swell propagating in the different directions.

Selection of Wave Gauge Stations in a Wave Flume

The present technique of wave resolution can be employed in the vicinity of reflective structure if the magnitude of reflection coefficients only is of concern. Figure 6 shows the variation of resolved, incident and reflected wave amplitudes against the distance of wave gauge from the face of submerged breakwater. The test was done with regular waves at the conditions same with those shown in Figs. 2 and 3. The test result indicates that the wave gauge may be set as near as 0.1 L to the reflective face. The dashed line for closed triangles and the dash-dot line for closed circles show the average values of a_R/a_S for the range of $x_1/L > 0.2$. The test was also carried out with irregular waves by shifting the wave gauge position from $x_1 = 1$ to 480 cm, while the wave gauge spacing was fixed at $\Delta\ell = 20$ cm. The wave spectra shown in Fig. 4 were taken from the data of this test. The reflection coefficient defined by Eq. 9 is found to vary little except at $x_1 = 1$ cm as shown in Fig. 7.

For the estimation of incident and reflected wave heights, on the other hand, wave gauges are required to be away from both the test structure and wave paddle. This is because the composite wave height H_S used in Eq. 10 fluctuates in the neighbourhood of a reflective boundary. The fluctuation of wave heights of irregular standing waves can be calculated with spectral information as demonstrated by Ishida [5]. For a component wave with the angular frequency of σ and wave number of k, the surface elevation of standing waves at the distance of x_1 from the reflective boundary is given as:
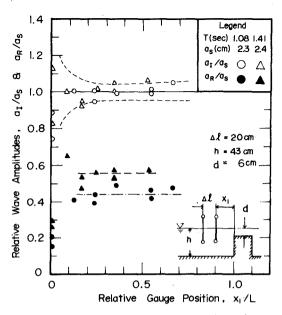
Fig. 6   Variations of Incident and Reflected Wave
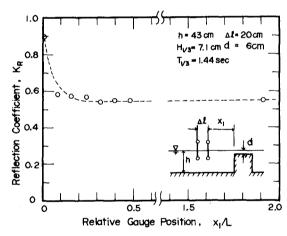   Amplitudes with Wave Gauge Position

Fig. 7   Variation of Reflection Coefficient of Irregular
         Waves with Wave Gauge Position

$$\eta = a_I \cos(kx_1 - \sigma t) + K_R a_I \cos(kx_1 + \sigma t)$$

$$= (1 + K_R) a_I \cos kx_1 \cos \sigma t + (1 - K_R) a_I \sin kx_1 \sin \sigma t$$

$$= \sqrt{1 + 2K_R \cos 2kx + K_R^2} \ \cos(\sigma t - \varepsilon_1), \tag{11}$$

where,

$$\varepsilon_1 = \tan^{-1} \frac{(1 - K_R) \sin kx_1}{(1 + K_R) \cos kx_1}. \tag{12}$$

The root-mean-square value of surface elevation of standing waves, $(\eta_s)_{rms}$, is calculated with the relation of Eq. 11 and the information of incident wave spectrum, $S_I(f)$, as

$$(\eta_s)_{rms}^2 = \int_0^\infty (1 + 2K_R \cos 2kx_1 + K_R^2) S_I(f) df. \tag{13}$$

The significant or any other representative height of irregular standing waves is then obtained as

$$H_S = \frac{(\eta_s)_{rms}}{(\eta_I)_{rms}} H_I. \tag{14}$$

Figure 8 is an example of the fluctuation of irregular standing wave heights; the test condition is the same with those of Figs. 4 and 7. The curves represent the result of calculation by Eq. 13 and 14. The incident wave spectrum was obtained from the measurement of progressive waves without a reflective structure. The reflection coefficient of 1.0 and 0.55 were used for the case of a high vertical wall and that of sub-merged, upright breakwater, respectively. The observed heights of significant waves are represented with the open and closed circles. Though the observed heights are somewhat larger than the calculation possibly because of the multi-reflection and nonlinearity effects, the magnitude of fluctuation is quite in agreement with the calculation. Such the fluctuation of standing wave heights directly affects the estimate of incident and reflected wave heights as the consequence of Eq. 10. The fluctuation becomes negligibly small, however, at the distance of more than one wavelength. A similar phenomenon will take place in front of a wave paddle with the high reflectivity. Therefore, the wave gauges for wave resolution are recommended to be located at the distance of more than one wavelength from both the test structure and wave paddle.

ACCURACY OF THE ESTIMATES OF INCIDENT AND REFLECTED WAVE HEIGHTS

Possible Sources of Inaccuracy

There are several sources of inaccuracy in the present resolution technique. They are:

1) Deviation from the dispersion relation of Eq. 6 due to nonlinear effect and others,

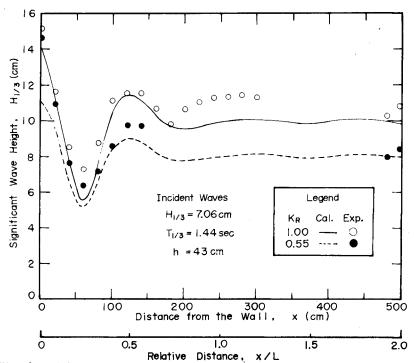2) Existence of nonlinear harmonic terms in progressive waves,

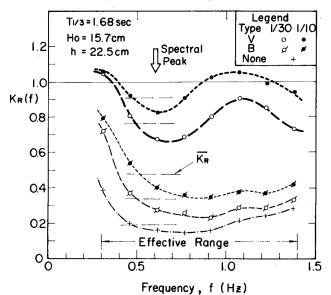Fig. 8   Undulation of Significant Wave Heights in front of Reflective Wall

Fig. 9   Frequency-wise Resolution of Reflection Coefficient of Seawalls

3) Generation of nonlinear interaction terms in standing waves,

4) Appearance of transversal waves and other disturbances in
    a wave flume,

5) Signal noises.

The dispersion relation of Eq. 6 is for the small amplitude waves.
The regular waves of finite amplitudes are known to deviate from that
relation. The wave number decreases for progressive waves [6,7], while
it increases for standing waves in relatively shallow water [8,9].
The existence of the deviation for wind waves has also been reported [10],
though not examined yet for mechanically generated irregular waves.
Any deviation from Eq. 6 leads to the inaccuracy in the estimates of a_I
and a_R in Eq. 5 because the resolution is based on the relative phase
difference of $k\Delta\ell$. The inaccuracy is greatest at the condition of $k\Delta\ell =$
$n\pi$ where $\sin k\Delta\ell = 0$ and smallest at $k\Delta\ell = (n+1/2)\pi$ where $\sin k\Delta\ell = 1$.
The divergence of a_I and a_R in Figs. 2 and 3 or $S_I(f)$ and $S_R(f)$ in Fig. 4
is due to the deviation of wave number from Eq. 6 to a large extent.

The second source of inaccuracy affects not the spectral peak of
irregular waves nor the fundamental component of regular waves but the
estimates of harmonic components. The regular waves of finite amplitudes are
accompanied by the harmonics which propagate with the same celerity with the
fundamental one to keep the wave profile permanent despite of their high
frequencies. For such harmonic components Eq. 6 does not apply and errors
may be evoked. The situation in a wave flume is more complicated, however.
There are free waves with the frequencies of harmonics and nonlinear
interacting waves, both of which contribute to the generation of travelling,
secondary waves in a wave flume [11, 12, 13]. Similar situation exists in
case of irregular wave experiments, though the analysis of nonlinear
harmonics and their behaviour is difficult. At present, we should content
ourselves by taking caution in the interpretation of the resolution results
in the range of harmonic components.

When two trains of finite amplitude waves interact such as in the case
of wave reflection, there appear nonlinear interaction terms the frequencies
of which are the sums and differences of fundamental and harmonic components.
Calculation of the third order solution of partial standing waves [9] has
shown the generation of the terms of $\cos[(\bar{k} + 2\Delta k)x + 3\sigma t]$ and $\cos[(3\bar{k} + 2\Delta k)x$
$\mp \sigma t]$ in which $\bar{k}$ and Δk are the mean and difference of the wave numbers of
incident and reflected waves in the standing wave system for the angular
frequency of σ. The phase velocities of these nonlinear interaction terms
are different from those of free waves having the angular frequency of σ
or 3σ, and therefore they become a source of inaccuracy in wave resolution.
Similar phenomenon occurs in irregular waves having frequency spectra, though
detailed analysis will be complicated.

An indication of such nonlinear effects can be seen in Fig. 9, which
shows the frequency-wise representation of reflection coefficient of a sea-
wall with vertical face (type V) and a seawall with a mound of artificial
concrete blocks (type B) on the bottom slope of 1 in 10 and 1 in 30.
Thin dash-dot lines indicate the overall reflection coefficient estimated
by Eq. 9 for the effective range of resolution. Humps of $K_R(f)$ around
twice the spectral peak frequency for the type V seawall may be due to
the nonlinear effects. When the reflection coefficient is low such as
for the type B seawall or the case of no seawall, the humps become insigni-
ficant. Experiments with waves of longer periods have exhibited another

humps around thrice the spectral peak frequencies. Therefore, the frequency-wise representation of reflection coefficient should be treated with due regard for the nonlinear effects. The employment of the overall reflection coefficient by Eq. 9 is based on this consideration.

Estimation of Accuracy of the Resolution Technique

Indication of the accuracy of the present technique is seen in Figs. 2, 3, and 6 as the dispersions of resolved amplitudes. In case of progressive waves and partial standing waves, the dispersion is of the order of $\pm$ 5% except for the diverging zone, while it becomes about two times in the case of standing waves. These dispersions are partly due to the variability of waves in a laboratory flume, and the error involved in the resolution technique is considered less than those indicated in these figures.

The effect of nonlinear terms of finite amplitude waves upon the wave resolution is difficult to quantitate. It should he mentioned here that the conventional method of estimating the reflection coefficient with the observed heights of maxima and minima of partial standing wave systems is much suceptible to the nonlinear effects. For example, the conventional method tends to yield an apparent reflection coefficient of low value for a highly reflective structure and a correction is required [9]. The conventional method is essentially for the fundamental frequency component of small amplitude waves. It cannot detect other associated components such as the harmonics, but it is influenced hy them instead.

The overall accuracy of wave height estimation is considered rather small for incident waves. Suppose that the significant height of H_S = 20 cm was measured for an irregular standing wave system and the reflection coefficient of the structure in test is 0.6. The true incident wave height is H_I = 17.1 cm by Eq. 10. If the wave resolution have produced the estimate of K_R = 0.7 by some reason, the estimate of H_I would he 16.4 cm, which is smaller than the true value by 4%. When the reflection coefficient is small, the error in the estimate of incident wave height becomes negligible.

EXAMPLES OF APPLICATIONS

The resolution technique has been employed in the authors' laboratory for irregular wave experiments since 1973. A series of wave overtopping tests have been carried out for seawalls with vertical faces and other types of seawalls [14]. Trains of irregular waves of about 200 waves long were generated and exerted upon model seawalls. The total amount of over-topped water was measured for each wave train, which yielded the rate of wave overtopping per second per unit length of seawall. At the same time, wave records of composite waves were taken by the two gauges in the offshore, and the incident and reflected wave heights were estimated from those records by the present technique. Figure 9 for the frequency-wise reflection coef-ficient is an example of the results of wave overtopping tests. Without the use of the resolution technique, the tests would have been much laborious since a number of short wave trains would have had to be employed to avoid the multi-wave-reflection problem. The tests have produced a set of twelve diagrams for the estimation of wave overtopping rate of seawalls under irregular wave actions, covering the full range of water depth from the offshore to the foreshore.
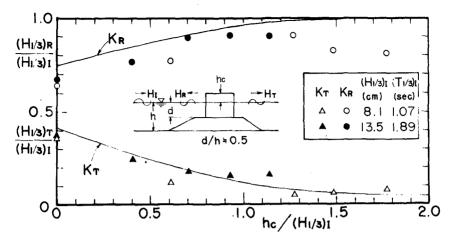
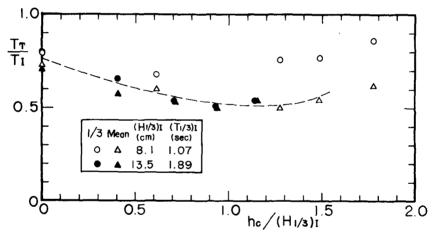Fig. 10   Transmission and Reflection Coefficients of a Composite Breakwater

Fig. 11   Change of Wave Periods by Wave Transmission
over a Composite Breakwater

Another example of wave tests for continuous wave actions is the wave transmission characteristics of a composite-type breakwater, which consists of a caisson rested upon a rubble mound. When the crest of breakwater is not high enough, some waves overtop it and new waves are generated behind it. The characteristics of transmitted waves by irregular wave actions can be revealed by experiments with continuous runs only. Figure 10 is a result of such experiments [15]. The ratio of significant height of transmitted waves to the incident significant wave height, $(H_{1/3})_T/(H_{1/3})_I$, as well as the reflection coefficient are plotted against the ratio of crest height to incident wave height, $h_c/(H_{1/3})_I$. The curves are those of regular waves previously formulated by the senior author [16]. The transmitted waves have two distinct properties. The one is the distribution of wave heights being broader than the Rayleighan. The second is the wave period being shorter than the incident waves. Figure 11 shows the latter characteristic. Both the mean and significant wave periods decrease to 50 to 80% of the incident wave periods.

The present resolution technique is also effective to detect the enhancement of harmonic components of waves through the interaction with structures. Figure 12 is one of such examples. A slit caisson with the opening ratio of 20% was tested for wave absorbing characteristics. As listed in the figure, the reflected wave height was estimated as 4.9 cm for the incident waves of $(H_{1/3})_I = 10.3$ cm and $T_{1/3} = 2.65$ sec, and the overall reflection coefficient was 48%. An interesting feature of the slit caisson is that it enhances the third harmonic component when it reflects waves. The feature has been predicted by Mei, Liu, and Ippen [17] in general form and is demonstrated in Fig. 12 as a hump of reflected wave spectrum around $3 f_o = 1.05$ Hz, where $f_o = 0.35$ Hz corresponds to the spectral peak of incident waves. Though a caution should be taken in the interpretation of resolved harmonic components as discussed earlier, the result of Fig. 12 is judged to represent actual generation of the third harmonics because it is not observed in the spectrum of incident waves and the overall reflection coefficient is relatively low.

The enhancement of odd harmonic components by wave reflection was more conspicuous when the slit caisson was tested for regular waves. The undulation of wave heights by formation of partial standing wave system was obscured by the presence of odd harmonics and the conventional method for the measurement of reflection coefficient had difficulty to obtain the correct value of reflection coefficient.

The application of the present technique of wave resolution is not confined to the above examples. It is applicable to any wave test with regular or irregular trains of waves. Though the question of wave nonlinearity effects remains to be clarified, it will provide the most needed means to measure the coefficient of reflection of irregular waves.

CONCLUSIONS

A technique to resolve the incident and reflected waves from the records of composite waves has been proposed. Examination of the technique with wave tests has shown the followings:

1) The wave resolution is not possible around the condition of $\Delta \ell/L$ = n/2 where n = 0, 1, 2, ... As a guideline, the wave resolution may be performed in the range of $0.05 < \Delta \ell/L < 0.45$.
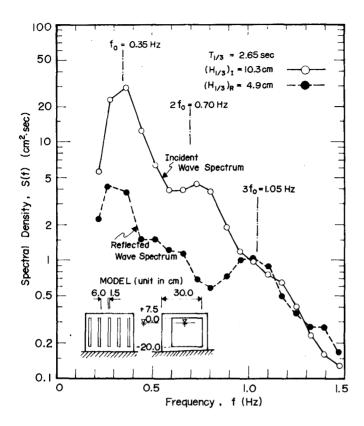
Fig. 12 Example of Spectral Resolution of a Slit Caisson

2) The wave gauges are recommended to be located at the distance of
    more than one wavelength from the test structure and wave paddle
    in the irregular wave test. In the regular wave test, the wave
    gauges may be set as near to the structure as at the distance of
    0.2 L.

3) There remains the problem of nonlinear wave interaction which
    may affect the accuracy of the wave resolution technique.

4) The technique is effective in detecting the enhancement of odd
    harmonics in the wave reflection by a structure such as a slit
    caisson.

     The authors sincerely express their thanks to Messrs. Yasuharu Kishira
and Osamu Kikuchi, members of the authors' laboratory, for their earnest
cooperation in carrying out the experimental verification.

REFERENCES

1) Kajima, R.: Estimation of incident wave spectrum in the sea area
     influenced by reflection, Coastal Engineering in Japan, Vol. 12,
     J.S.C.E., 1969, pp.9–16.

2) Thornton, E. B. and R. J. Calhoun: Spectral resolution of breakwater
     reflected waves, Proc. A.S.C.E., Vol. 98, No. WW4, 1972, pp.443–460.

3) Goda, Y. and K. Nagai: Investigation of the statistical properties of
     sea waves with field and simulation data, Rept. Port and Harbour
     Res. Inst., Vol. 13, No. 1, 1974, pp.3–37,(in Japanese).

4) Coda, Y.: Estimation of wave statistics from spectral information,
     Proc. Int. Symp. on Ocean Wave Measurement and Analysis, New Orleans,
     1974, Vol. 1, pp.320–337.

5) Ishida, A.: Transformation of power spectra of wind-generated waves
     caused by reflection, Coastal Engineering in Japan, Vol. 15, J.S.C.E.,
     1972, pp.25–33.

6) Stokes, G. G.: On the theory of oscillatroy waves, Trans. Camb. Phil.
     Soc., Vol. 8, 1847.

7) Skjelbreia, L.: Stokes' third order approximation, Tables of function,
     Council on Wave Research, The Engineering Foundation, Berkely, 1958.

8) Tadjbaksh, I. and J. B. Keller: Standing surface waves of finite ampli-
     tudes, Jour. Fluid Mech., Vol. 8, 1960, pp.442–451.

9) Goda, Y. and Y. Abe: Apparent coefficient of partial reflection of finite
     amplitude waves, Rept. Port and Harbour Res. Inst., Vol. 7, No. 3,
     1968, pp.3–58.

10) Hidy, G. M. and E. J. Plate: Wind action on water standing in a labora-
     tory channel, Jour. Fluid Mech., Vol. 26, 1966, pp.651–687.

11) Hansen, J. B. and I. A. Svendsen: Laboratory generation of waves of
     constant form, Proc. 14th Coastal Engg. Conf., Copenhagen, 1974,
     pp.321–339.

12) Hulsbergen, C. H.: Origin, effect and suppression of secondary waves,
     Proc. 14th Coastal Engg. Conf., Copenhagen, 1974, pp.392–411.

13) Ishida, A.: On the characteristics of splitting solitons in shallow waters, Proc. 22nd Coastal Engg. Conf. in Japan, J.S.C.E., 1975, pp.41-46, (in Japanese).

14) Goda, Y., Y. Kishira, and Y. Kamiyama: Laboratory investigation on the overtopping rate of seawalls by irregular waves, Rept. Port and Harbour Res. Inst., Vol. 14, No. 4, 1975, pp.3-44, (in Japanese).

15) Goda, Y., Y. Suzuki, and Y. Kishira: Some experiences in laboratory experiments with irregular waves, Proc. 21th Coastal Engg. Conf. in Japan, J.S.C.E., 1974, pp.237-242, (in Japanese).

16) Goda, Y.: Re-analysis of laboratory data on wave transmission over breakwaters, Rept. Port and Harbour Res. Inst., Vol. 8, No. 3, 1969, pp.3-18.

17) Mei, C. C., P. L-F. Liu, and A. T. Ippen: Quadratic loss and scattering of long waves, Proc. A.S.C.E., Vol. 100, No. WW3, 1974, pp.217-239.

APPENDIX: MULTI-REFLECTED WAVES IN A LABORATORY FLUME

As described in the text, waves in a closed, laboratory flume may travel many times between a reflective model structure and the wave paddle as the result of wave reflections at the both boundaries. This composes a multi-wave-reflection system. Let the amplitude of initially generated waves be denoted by a_o, the reflection coefficients of the test structure and wave paddle by r and R, respectively, and the distance between them by ℓ. Then the wave profile of multi-wave-reflection system can be expressed as an infinite series of

$$\frac{\eta}{a_o} = \cos(\sigma t - kx) + R\cos(\sigma t + kx - 2k\ell)$$

$$+ rR\cos(\sigma t - kx - 2k\ell) + rR^2\cos(\sigma t + kx - 4k\ell)$$

$$+ r^2R^2\cos(\sigma t - kx - 4k\ell) + r^2R^3\cos(\sigma t + kx - 6k\ell)$$

$$+ \cdot \cdot \cdot \cdot, \tag{A.1}$$

where η is the surface elevation of waves, σ is the angular frequency of $2\pi f$, and k is the wave number of $2\pi/L$. The infinite series can be summarized after a few manipulations as a closed form of

$$\eta = \frac{a_o}{\sqrt{1 - 2rR\cos 2k\ell + r^2R^2}} \{\cos(\sigma t - kx + \theta) + R\cos(\sigma t + kx - 2k\ell + \theta)\}$$

where,

$$\tag{A.2}$$

$$\theta = \tan^{-1}\{\frac{rR\sin 2k\ell}{1 - rR\cos 2k\ell}\} \tag{A.3}$$

This proves the formation of two trains of waves propagating in the opposite directions as the result of multi-wave-reflections.